Separation Science and Technology
Publication details, including instructions for authors and subscription information:
http://www.informaworld.com/smpp/title~content=t713708471

Compressibility of Paniculate Structures in Relation to Thickening, Filtration, and Expression—A Review

Frank M. Tiller[a]; Charles S. Yeh[a]; W. Francis Leu[b]
[a] Department of Chemical Engineering, University of Houston, Houston, Texas [b] Rohm and Haas Company, Bristol, Pennsylvania

To cite this Article Tiller, Frank M. , Yeh, Charles S. and Leu, W. Francis(1987) 'Compressibility of Paniculate Structures in Relation to Thickening, Filtration, and Expression—A Review', Separation Science and Technology, 22: 2, 1037 — 1063
To link to this Article: DOI: 10.1080/01496398708068998
URL: http://dx.doi.org/10.1080/01496398708068998

SEPARATION SCIENCE AND TECHNOLOGY, 22(2&3), pp. 1037-1063, 1987

Compressibility of Particulate Structures in Relation to Thickening, Filtration, and Expression — A Review

FRANK M. TILLER and CHARLES S. YEH

DEPARTMENT OF CHEMICAL ENGINEERING
UNIVERSITY OF HOUSTON
HOUSTON, TEXAS 77004

W. FRANCIS LEU

ROHM AND HAAS COMPANY
P. O. BOX 584
BRISTOL, PENNSYLVANIA 19007

ABSTRACT

Compressibility of cakes is basic to separation of solids from slurries. Cake compression is caused by collapsing, particulate structures in which particles are forced into existing voids. Stresses causing the collapse arise from unbuoyed weight of solids in thickeners, radial acceleration in centrifuges, frictional pressure drop in filters, and mechanical forces in press belts and membrane actuated filters. Compressibility is a function of particle size and shape and the degree of aggregation.

Flow through very compressible cakes produces a highly non-uniform structure with a tight skin of low porosity next to the supporting medium. This skin leads to adverse effects in which increasing filter pressure has little effect on flow rate or average porosity. Similarly increasing the squeezing pressure indefinitely in expression has little effect upon the rate of removal of liquid.

SOLID-LIQUID SEPARATION

Solid-liquid separation (SLS) includes clarification, thickening, cake filtration, centrifugation, washing, and expression. Chemical and physical pretreatment of slurries also is an integral part of these separations. Closely allied to SLS are rheological behavior of suspensions, slurry transport, and biological processes involved in environmental protection.

Relative movement of solid and liquid constitutes the basic phenomena underlying separation of particles from liquids. The principal stages of SLS can be classified as follows:

1. Pretreatment generally for increasing effective particle size
   a. Chemical treatment through coagulation and flocculation
   b. Physical treatment
2. Thickening and clarification
   a. Gravity sedimentation
   b. Centrifugal classification in hydrocyclones
3. Separation
   a. Gravity separation, screening
   b. Pressure and vacuum filtration
   c. Centrifugal filtration
   d. Centrifugal sedimentation
   e. Filter thickening in delayed cake operations
4. Post treatment
   a. Displacement and dilution washing
   b. Deliquoring
      (1) Utilization of high pump pressure
      (2) Hydraulic deliquoring with reverse flow
      (3) Mechanical expression
      (4) Drainage
   c. Membrane processes for improving filtrate quality

All SLS operations involve flow through compressible porous cakes. The cake structure as reflected by variation of local values of porosity and permeability with distance and the process variables - pressure drop or rotational speed of centrifuges, flow rates, and average porosity - are fundamental to both practical and theoretical considerations.

FLOW THROUGH COMPRESSIBLE, POROUS BEDS

A typical separation process begins with a treated suspension in which the particulates may be dispersed as individual units or combined into an endless variety of aggregates. A cake or sediment is formed with a structure capable of sustaining stress. Liquid and fine particles flow through the pores formed by the structure. The beds may be incompressible as in preconsolidated petroleum reservoirs, aquifers, or cakes formed from large

particles; or they may be compressible when flocs and aggregated fine particles are deposited. Fine particles flowing through the interstices may be deposited or resuspended depending upon the relative magnitude of liquid shear and adhesive forces binding the fine particulates to larger members of the structural assemblage. Particulate structures vary enormously in resistance to compressible forces depending on the internal arrangement of the individual particles.

The behavior of compressible, porous beds is fundamental to the types of SLS operations. Even in thickeners, the settling characteristics of the freely sedimenting particles is of less importance than those of the compressed sediment. Although free settling generally controls the functioning of a gravity clarifier, the relative flow of solids and liquid in the compression zone of a thickener determines the solid and liquid fluxes and the sediment height necessary to maintain the desired solids under flow concentration. In filters, centrifuges, and expression devices, porosity and permeability of the cakes are the major determinants of operating behavior.

STRUCTURE OF PARTICULATE BEDS

Structural change through particulate rearrangement is effected by stresses transmitted at points of contact. Stress results from externally applied loads, gravitational and centrifugal forces, and from accumulated drag on particles due to frictional flow of liquid. The initial structure laid down under a null stress depends upon the microscopic properties of (1) particle size, (2) particle shape, and (3) degree of aggregation. Suspension concentration is a secondary variable having less importance. Agitation, vibration, and shear forces can have larger effects but are usually minimized in testing procedures.

Figure 1 provides a general picture of the solidosity (volume fraction of solids) as a function of particle size and other parameters. The open circles represent values found in the literature, and the black circles are values obained in our laboratories. For large particles (roughly above 20-50 microns), interparticle forces are small compared to gravitational forces; and aggregate formation is not an important factor. Large spherical particles of narrow range tend to form beds having volume fractions of solids in the range of 0.60-0.65 as shown by line BC. The behavior of small spherical particles (under 10-20 microns) is dependent upon the relationship between repulsive forces due to surface charge and attractive London-van der Waals forces. Strong repulsive forces resulting from high surface charges or zeta potential prevent particles from mutual attachment. Consequently, loose flocs are not formed, and the particles in suspension remain dispersed. Repulsive interparticle forces come into play at molecular dimensions and produce a "lubricating" effect which permits even fine particles in the sub-

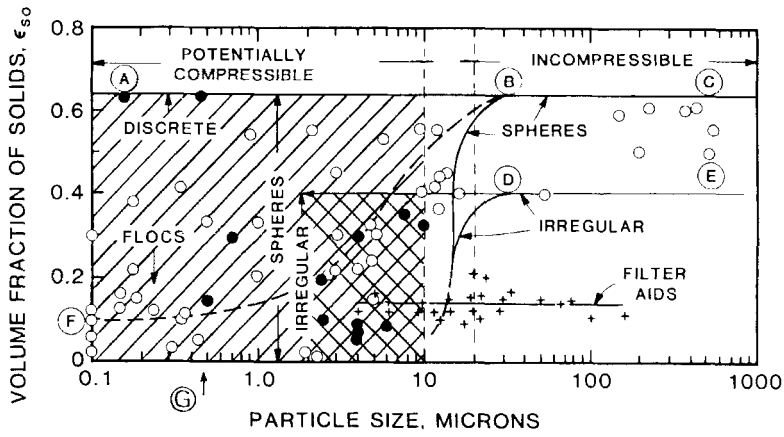

Figure 1. Volume fraction of solids (solidosity) in relation to particle size, shape, and degree of aggregation.

micron range to settle past one another and form a relatively dense, incompressible structure. In Fig. 2, the first layers of a bed of polystyrene particles having a high zeta potential are shown. The bed has a porosity of 0.37 (Bridger, et al., 1983). Thus spherical particles tend to form similar structures with the same porosity independent of particle size. Line ABC corresponds to spheres of all sizes and represents the normal maximum solidosity of a bed of uniform or randomly distributed spherical particles. Higher solid contents can be obtained with bi or trimodal distributions.

The line DE represents an irregular class of particles which has a lower volume fraction of solids than spheres. The large particles falling along DE lead to incompressible cakes. Among the most irregular of particles are diatomaceous and perlite filter aids with solidosities less than 0.2. They are shown at the bottom right of Fig. 1.

As particle size decreases and the ratio of surface area to volume increases, both repulsive and attractive forces become large in comaprison to gravitational effects. When London-van der Waals attractive forces prevail, particles which approach one another in suspension mutually adhere and form dendritic, tree-like structures or flocs. Each of these sets of aggregated particles possesses its own multiparticle arrangement. They deposit as highly porous, compressible cakes. A possible particulate structure as initially deposited is illustrated in Fig. 3.

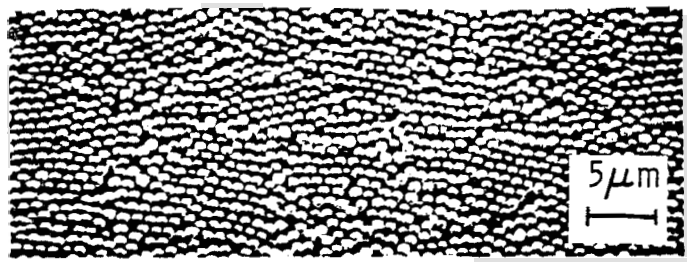

Figure 2. Discrete polystyrene particles with a porosity of 0.37, Bridger et al. (1983).

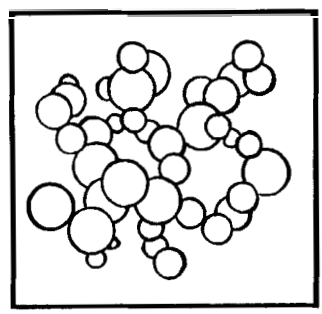

Figure 3. Aggregated particles in suspension.

When strong attractive interparticle forces or bridging mechanisms due to high molecular weight linear polymers or polymerized metal hydroxides (Al^{+++} or Fe^{+++}) are present, loose flocs are formed. Highly flocculated slurries encountered in wastewater and primary and activated sludges produce deposits which may have 90-95% voids by volume and require dewatering. When inorganic coagulants and high molecular weight organic flocculants are used, large flocs with characteristic dimensions of millimeters may settle rapidly and be removed by gravity or vacuum filtration. Loose structures which retain significant quanitities of liquid are frequently deliquored with press belts, recessed plates equipped with air or hydraulically actuated membranes, and high-pressure (up to 1.4 MPa (200 psi)) plate and frame or recessed plate filters.

Figure 1 is divided into two regions representing large particles forming incompressible beds and small particles which potentially yield compressible structures. The singly cross-hatched region covers the behavior of fine spherical particles which form cakes with solidosities ranging from 0.02-0.65. The doubly hatched region pertains to irregular particles whose shape leads to line DE as the maximum volume fraction of solids for a non-flocculated system. The range of solidosities is smaller than that of the spheres.

With large particles, shape is the sole factor determining porosity. The degree of aggregation plays the dominant role for small particles. The actual transition from "large" to "small" sizes depends principally on shape, the Hamaker constant as it affects the London-van der Waals forces, and the liquid and solid densities. Agitation and shear forces are significant in determining both formation and breakup of flocs in suspension. Slurry flow patterns at points of deposition in filters significantly affect cake structure. Suspension concentration has an important effect upon the porosity of each surface layer as first deposited and then covered by successive waves of particles. Dilute slurries lead to more compact beds while concentrated suspensions produce open structures. With high concentrations, particulates tend to bridge and form arches whereas dilute suspensions permit individual particles to penetrate deeply into the medium or cake without interference from nearby neighbors.

COMPRESSIBILITY

Compressibility is a measure of the degree of structural collapse brought about by compressive stresses. It depends upon the difference between the solidosities (or porosities) of cakes formed from dispersed and flocculated sets of particles. For example, two particles represented by black dots and having sizes indicated by the arrow labeled G correspond to (1) an incompressible (or nearly so) cake with a solidiosity about 0.63 and (2) a compressible bed with solidosity equal to 0.15. SLS operations of sedimentation, filtration, and centrifugation involve fluid flow through porous particulate beds which are usually compressible. Solids in the flow field are subjected to both form and frictional drags which result in cake compression. Failure of the particle structure and individual particle deformation are the principal elements of consolidation. Degradation of particle aggregates with movement of particles into open spaces constitutes the major non-elastic mechanism during cake formation. In expression operations involving relative high pressures, particles may deform or be crushed. Particle deformation depends on the nature of surface stresses and the elastic properties of the solid. Reasonably "hard" particles under low stress probably undergo only minor shape change.

EMPIRICAL CONSTITUTIVE EQUATIONS

The behavior of a compressible, porous bed depends mathematically on the solution of three sets of coupled differential equations. These equations, which appear in macroscopic form, have their origin in microscopic phenomena involving local conditions. In the present state of the art, a substantial amount of empirical simplification enters the theoretical formulations.

The three sets of equations cover (1) liquid phase, (2) solid phase, and (3) fine particles migrating in the liquid. These equations are:

1. Darcian-type equations relating the velocity of the liquid relative to the solids to the pressure gradient.
2. Stress-strain relations describing the collapse of the particulate structure when subjected to load.
3. Equations governing the transport and adhesion of migrating fine particles.

In addition, the equation of continuity enters in terms of the flowing liquid, the solids forming the particulate structure, and the migrating fine particles. We shall neglect the migrating fine particles and assume that members of the assemblage remain within the group after deposition.

When incompressible beds are involved, the microscopic differential equations lead to Darcy's equation with constant permeability. However, in compressible beds, the stresses developed in the solid matrix lead to deformation and compression. In turn, the pores undergo geometrical modifications affecting the flow fields and the permeability. The deformation of the particle structure contains both inelastic and elastic components, with the former predominating.

Power functions represent the chief form of empirical equations used for relating the permeability K, the specific flow resistance α, the porosity ε, and the solidosity ε_s ($\varepsilon + \varepsilon_s \equiv 1$) as functions of the effective pressure p_s.* One useful set of equations consists of (Tiller and Leu, 1980)

*Definition of K and α are based on the following forms of the Darcy equation

$$q = \frac{K}{\mu}\frac{dp_L}{dx} = \frac{1}{\mu\alpha}\frac{dp_L}{d\omega}$$

where ω the volume of dry solids/unit area is related to x by $d\omega = \varepsilon_s dx$. This definition of α depends upon volume of solids rather than the usual form which employs mass/unit area. The authors consider the form based on volume to be more valuable practically than the traditional specific flow resistance.

$$\varepsilon_s = \varepsilon_{so} (1 + p_s/p_a)^{\beta} \quad (1)$$

$$\alpha = \alpha_o (1 + p_s/p_a)^{n} \quad (2)$$

$$K = K_o (1 + p_s/p_a)^{-\delta} \quad (3)$$

where ε_s = volume fraction of solids under a solid effective pressure p_s. The term p_a is an empirical parameter devoid of physical meaning. The quantities α and K are related by

$$\alpha K \varepsilon_s = 1 \quad (4)$$

It can be shown that $\delta = n + \beta$ by combining Eqns. 2 and 3 in accord with Eqn. 4.

The exponents β, n, and δ are compressibility coefficients. As a crude rule, we generally assume $n = 4\beta$ in the absence of experimental information. We use the following tentative limits and descriptive terms to categorize cakes:

Cake Description	Value of n, δ
Incompressible	0
Slightly compressible	0 -0.25
Moderately compressible	0.25-0.6
Highly compressible	0.6 -1.0
Super compressible	1.0 -

When n is above approximately 0.6-0.7, the ranges over which the approximations in Eqns. 1-3 are valid decrease substantially. The compressibility parameters provide information about how fast ε_s, α, and K change with pressure. The magnitude of the permeability is a measure of the difficulty of filtration. A rough classification follows:

Description	Value of K, m^2
2.0 in pipe in laminar flow	10^{-5}
Sand bed	10^{-11}
Very easy to separate, 1.0 Darcy	10^{-12}
Easy to separate	10^{-13}
Moderate	10^{-14}
Difficult, 1.0 milli-Darcy	10^{-15}
Very difficult, colloidal silica, attapulgite	10^{-16}

FRICTIONAL DRAG ON PARTICLES

As liquid flows through a compressible, filter cake, the friction drop leads to compression of the particle structure. The compression process results from nearly irreversible movement of particles into voids; and at high pressures, particle deformation

and breakage occur. Any attempt to link the cake compression to pseudo elastic behavior will yield only minimal results. Treating the bed as a continuum is convenient but hides the fundamental phenomena underlying cake behavior. Stress transmission from particle to particle or floc to floc is a poorly understood three-dimensional problem even when macroscopically unidirectional flow is involved. We present a simplified analysis of the relation of drop in liquid pressure in relation to the rise in effective pressure.

Figure 4 displays the nomenclature and general arrangement for a compressible filter cake. (Flow occurs from right to left). The porosity is at its maximum value at the cake surface and at its minimum at the medium. Individual particles of the cake are assumed to be in point contact; and surface forces resulting from friction create internal stresses which are communicated to other particles sequentially through the network. We envision a membrane which curves around particles and lies entirely in the fluid phase; and we assume that the particles are small as compared to cake thickness. The x component of a force acting on the membrane is then Ap_L.

Each particle is subject to frictional and form drag which in turn generate internal forces which are communicated from particle to particle at points of contact. An ideal particulate model consists of particles which have point as opposed to area contact. Where area contact exists, the equivalent of tube walls pass

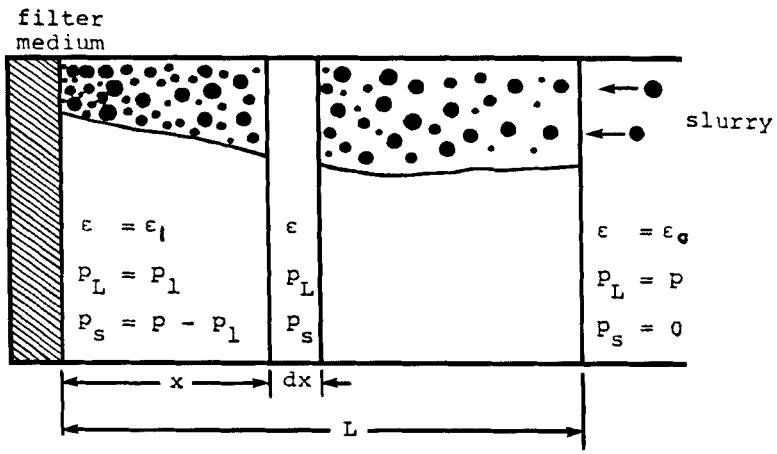

Figure 4. Schematic diagram of a filter cake.

through the porous bed as exemplified by porous metals and ceramic filters. In the ideal particulate bed, the liquid pressure is assumed to be effective over the entire surface. As the liquid flows around a particle, the normal pressure and tangential drag components can be integrated over the entire surface.

A force balance over the distance L-x (Figs. 4 and 5) assuming negligible inertial effects can be written as

$$Ap_L + F_s = Ap \tag{5}$$

where p is the filtration pressure.

Equation 5 rests on the assumption that there is a point contact among particles and that the liquid pressure integrated over an undulating unbroken surface yields the first term in Eqn. 5. The term F_s represents the accumulated frictional drag arising from the total particulate surface. It is communicated from particle to particle at points of contact. A fictitious pressure (effective or compressive drag pressure) is defined by $p_s = F_s/A$. Dividing Eqn. 5 by A yields

$$p_s(x,t) + p_L(x,t) = p(t) \tag{6}$$

The format of Eqn. 6 indicates that p_s and p_L are functions of both time and location, but that p is a function of time only. It

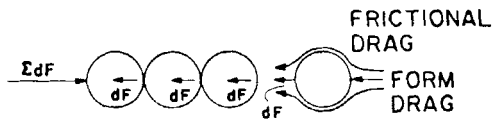

ACCUMLATION OF FRICTION AND FORM DRAGS

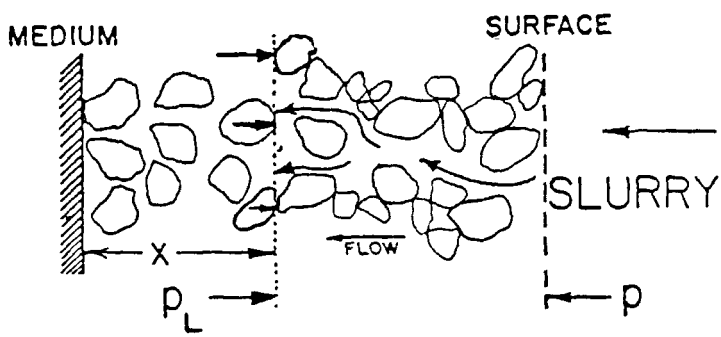

Figure 5. Stresses in a particulate bed.

should be noted that the area "A" is the full cross section area of filtration without adjustment for the areas of contact. The symbol "p_s" thus does not represent a specific and real pressure but is one (similar to "effective pressure" in soil mechanics) which permits mathematical simplifications.

Finally, taking differentials at constant time, we have

$$dp_s + dp_L = 0 \tag{7}$$

This equation allows us to replace dp_L in Darcy's equations by $-dp_s$. Inasmuch as the volume fraction of solids, permeability, and specific flow resistance are functions of p_s, a change from p_L to p_s is desirable. Unfortunately in radial flow as involved in centrifuges and with cakes deposited on tubular surfaces, the force balance equations lead to more complicated differential equations (Tiller and Yeh, 1985).

Variation of the hydraulic and solid or effective pressures in a typical filter cake is illustrated in Fig. 6. At the surface of the cake, the effective pressure is zero as no drag on the particles has developed. Consequently, the surface layer of the cake is unstressed, and the porosity has its maximum value at that point. The porosity reaches a minimum at the medium where the effective pressure has risen to its maximum value and equals the pressure drop across the cake. Whereas the porosity at the cake surface theoretically remains the same regardless of the pressure drop, the porosity at the medium decreases as the pressure drop becomes larger.

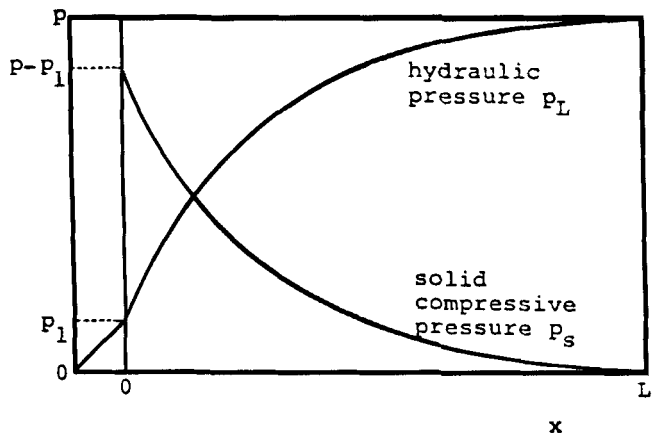

Figure 6. Variation of hydraulic and solid or effective pressures in a compressible filter cake.

FILTER CAKE BEHAVIOR

It is well-known that the porosity of a cake is not uniform, being a maximum at the cake surface and a minimum at the medium which serves as a support for the cake. In Fig. 7, porosity is shown as a function of the fractional distance through a filter cake produced under constant applied pressure. The three curves illustrate (1) an incompressible solid (uniform spheres in their most open packing), (2) moderately compressible materials like talc and a clay used for ignition (spark) plugs, and (3) a highly compressible material.

The solids forming the cake are compact and relatively dry at the medium, whereas the surface layer is in a wet and soupy condition. The porosity is at a minimum at the point of contact between the cake and medium, where $x = 0$, and at a maximum at the surface, $x = L$, where the liquid enters. The drag on each particle is communicated to the next particle; and consequently, the net solid compressive pressure increases as the medium is approached, resulting in decreasing porosity. The porosity for latex remains almost constant over 80% of the cake, and a resistant skin develops in the 20% of the cake closest to the medium. There would be little pressure drop over the portion of

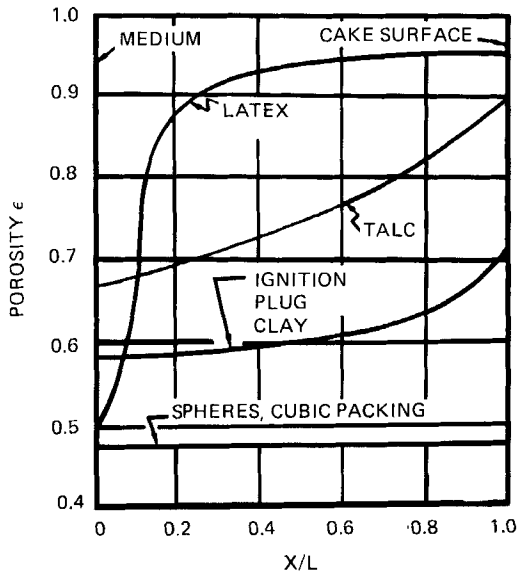

Figure 7. Porosity vs. fractional distance through cake.

the cake with high porosity. Lack of fluid drag on the particles accounts for the lack of consolidation.

The resistant skin is disadvantageous and is the cause of many problems in filtration. It leads to adverse effects on rate and average porosity with increasing pressure.

In Fig. 8, fractional pressure drop through cakes of varying compressibility is plotted as a function of fractional distance. Incompressible materials are represented by the 45° line. As the cake becomes more compressible, the relation between pressure and distance develops increasing curvature. For highly compressible beds, there is little pressure drop over the first portion of the cake. Most of the drop is concentrated over the resistant skin close to the medium. The relationship between pressure drop and porosity change can be seen by comparing the region in Fig. 7 where the porosity remains constant with the corresponding region of Fig. 8 where the pressure remains flat. Highly compressible cakes generally have high permeabilities at low pressure. However, their sensitive structures compares rapidly and produce the behavior illustrated in Figs. 7 and 8.

In Fig. 9, the flow rate/unit area is shown as a function of the pressure drop across the cake. The rate depends on the

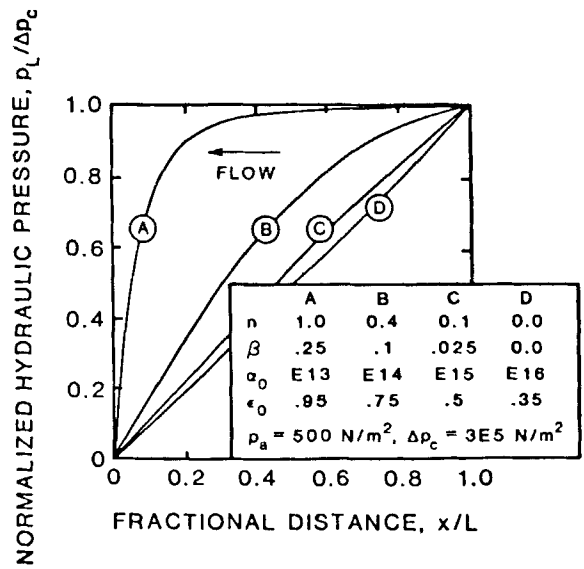

Figure 8. Pressure distribution in filter cakes.

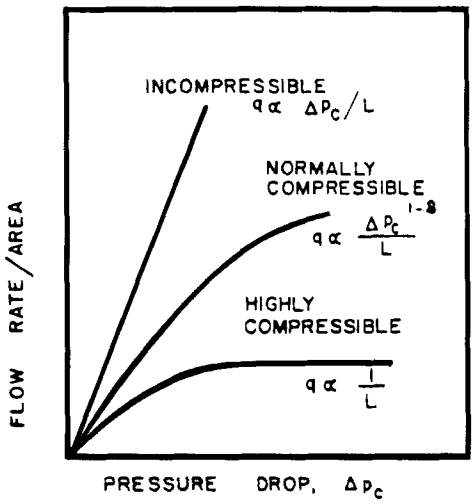

Figure 9. Flow rate/area vs. pressure drop across the cake.

compressibility coefficent δ or $n + \beta$ which relate the average specific resistance α_{av} and average volume fraction of solids ε_{sav} to the pressure drop Δp_c across the cake. For an incompressible material such as coarse sand, n and β are both zero, and the rate is directly proportional to the pressure drop and inversely proportional to the cake thickness.

Substances normally encountered in filtration practice involve values of δ ranging from 0.2 for filter aid to 0.6 for clays. The flow rate of such materials increases with less than the first power of Δp_c as illustrated. As δ approaches unity and $1-\delta$ tends to zero, the flow rate reaches a point where it is essentially independent of the pressure drop across the cake. As a practical matter, the flow rate for the highly compressible material shown in Fig. 9 would probably drop as pressure drop across the cake increases. High pressure would force the cake into the interstices of the medium thereby increasing the overall resistance more rapidly than the pressure and resulting in decreased flow rate.

Compressibility, high resistance of small particles, and blinding due to migration and deposition of colloids in both cake and medium represent the major obstacles to particulate separation. We generally consider five microns to be the size at which dispersed particles begin to cause serious rate problems. Particles with characteristic lengths in the one micron range are

so difficult to filter or centrifuge that it is necessary to consider other methods such as electrophoresis.

Inasmuch as increasing pressure is not effective in increasing rates with many materials such as slimes, other means must be sought for augmenting the rates. Among possible methods are:

1. Improve pretreatment methods
2. Grow larger crystals
3. Add filter aids
4. Decrease cake thickness by agitation or cross-flow
5. Adjust time of filtration in batch cycles to maximize average rate.

The effect of pump pressure on the final liquid content is significant in design and operation of filters. In Fig. 10, the average porosity is plotted as a function of the pressure drop across the cake. It is apparent that the applied pressure has little effect on the average porosity of the highly compressible latex once a pressure equal to about 10 psi (70 kPa) has been reached. The curves in Fig. 10 are deceptive in that visually there appears to be little difference among them. A better quantitative view can be obtained by plotting the void ratio

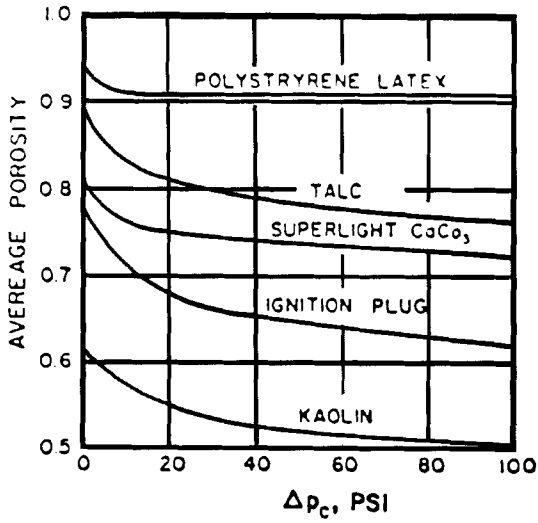

Figure 10. Average porosity vs. pressure drop.

instead of porosity or volume fraction of solids. The void ratio is defined as the volume of liquid per unit volume of solids. Since the solid volume remains constant during SLS, changes in the void ratio provide a measure of the liquid removed per unit of solid. The data from Fig. 10 have been replotted as void ratio vs. pressure drop across the cake in Fig. 11. The much larger amount of liquid removed from the cakes with high initial porosity in comparison with the initially more compact cakes is apparent.

A substantial difference exists between the talc and flocculated polystyrene latex which both start with high initial porosities. Under pressure filtration, the latex ceases to deliquor at a relative low pressure whereas the talc improves as the pump pressure continues to increase. The latex requires some type of mechanical expression such as a press belt or a pressure actuated membrane acting like a piston at the end of a filter cycle. The talc would deliquor reasonably with increasing pump pressure.

Figure 12 presents the data of Figs. 10 and 11 replotted as the fraction of liquid removed as a function of pressure drop across the cake. On the basis of the materials shown in Fig. 12, it would appear that increase in pump pressure has a rapidly decreasing effectiveness in liquid removal once it surpasses two atmospheres.

HYDRAULIC DELIQUORING

Inasmuch as increasing filtration pressure rapidly loses its effectiveness for deliquoring of filter cakes, other means must be sought for reducing liquid content. The skin, which is highly disadvantageous in direct filtration, can be used for deliquoring purposes during washing in a plate-and-frame filter press. Tiller and Horng (1983) demonstrated theoretically and experimentally that in washing with reverse flow through cakes the resistance skin acts as a piston to compress the cake.

The reverse flow process is illustrated in Fig. 13 where calculated values for three different degrees of compressibility are illustrated. Calculations were based on the dimensionless pressure p_s/p_a which appears in Eqns. 1-3. Values attached to the various curves represent the pressure drop across the cake in the washing mode $\Delta p_c/p_a$. The value of $\Delta p_c/p_a = 50$ corresponds to the pressure during filtration. The curves marked 5 and 100 represent pressures during reverse washing which are respectively one-tenth and twice the filtration pressure. The skin moves under action of the pump as shown in Fig. 13. The highly compressible material undergoes a large movement of the surface with substantial deliquoring. If a backwash pressure of 50 is employed, the cake surface moves from A to B. Thus, the cake thickness is reduced about 50%. Liquid fills that portion of the frame between A and B and must be drained for the process to be successful.

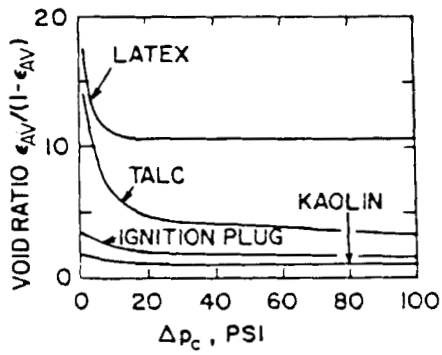

Figure 11. Void ratio vs. pressure drop across the cake.

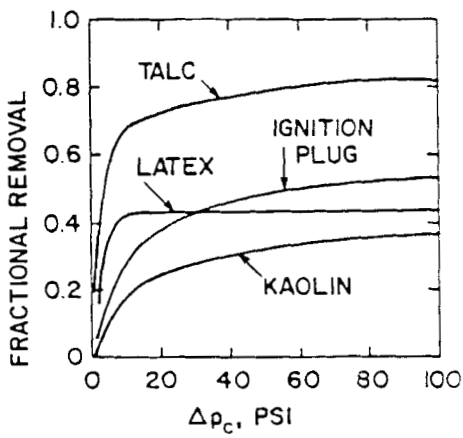

Figure 12. Fraction of liquid removed as a function of the pressure drop across the cake.

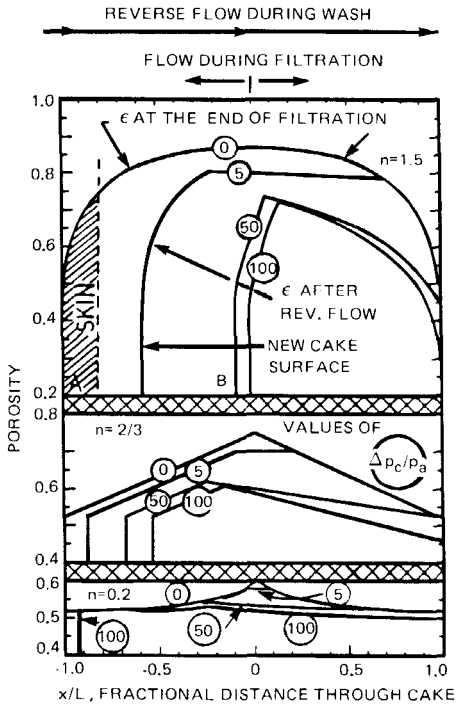

Figure 13. Porosity vs. fractional distance through cake in reverse deliquoring in a plate-and-frame filter press.

The reverse flow operation is mildly successful for the moderately and slightly compressible cakes. Its value lies in the fact that it offers great promise for those very compressible materials which respond poorly to normal practice.

In Fig. 14, experimental and theoretical values for deliquoring with reverse flow are demonstrated. In experiments, two separate cakes were formed under vacuum. One was then placed on top of the other to simulate cake formation in a plate-and-frame press. Liquid when then drawn through the two cakes in a

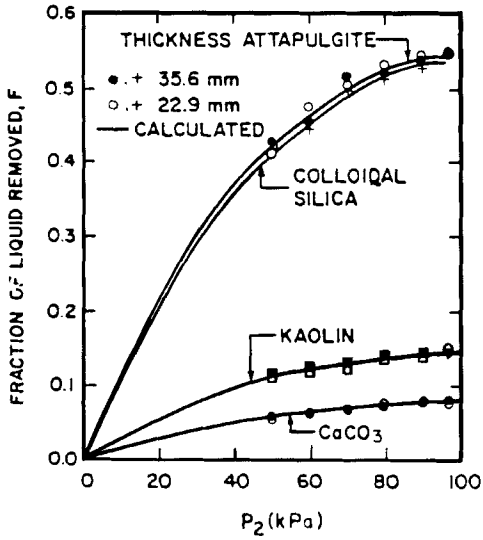

Figure 14. Fraction of liquid removed vs. deliquoring pressure in reverse deliquoring (Experimental results).

series in a manner analogous to washing in a plate-and-frame press. The relative amount of liquid removed for the highly compressible colloidal silica and the attapulgite was quite impressive.

MECHANICAL EXPRESSION

The use of membranes to compress cakes has become popular in recent years. In general, as pressure is built up, the ultimate porosity that can be reached is decreased. However, decreased porosity means increased resistance to flow, and the rate of expression of liquid is adversely affected by decreased permeability. Cakes in mechanical expression operations act very much like filter cakes.

In the theory of flow through compressible cakes, Tiller and Green (1973) demonstrated that the flow rate of a highly compressible material reached a constant value when the pressure drop exceeded some relatively low value. At that point,

resistance to flow increases in direct proportion to the pressure drop. The average porosity also reaches an essentially constant value at the same point. For the latex in Figs. 10-12, the rate would be expected to remain constant at about 1 atm where the removal of liquid from the cake ceases.

The same phenomenon occurs in mechanical expression. For highly compressible attapulgite, the average porosity (ε_{av}) vs. time curves as shown in Fig. 15 were essentially identical for pressures ranging from 1.7-24.7 MPa during the first 1 hour of expression. After that period of time, the porosities decreased further to their limiting values for the higher pressures. Figure 16 shows a plot of the average void ratio, e_{av}, vs. $t/\rho_s^2\omega_c^2$ with an expression pressure of 10.4 MPa. There is an significant drop of e_{av} at the beginning period. After about 12 $\rho_s^2\omega_c^2$ seconds, the average void ratio reaches its ultimate value. The unified curve in Fig. 16 indicates that the expression time is proportional to the square of the amount of solids at constant pressure expression.

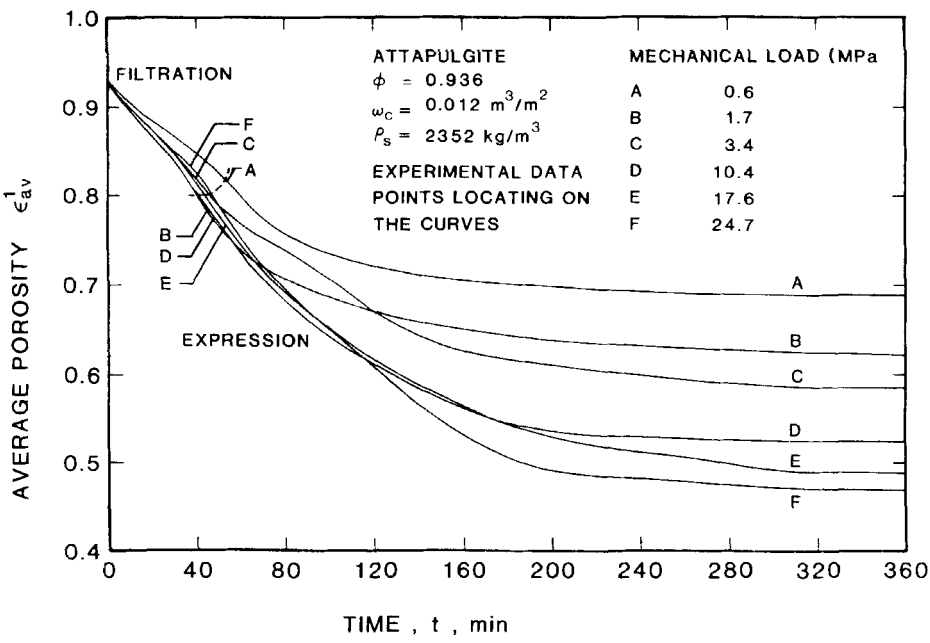

Figure 15. Average porosity vs. time in expression.

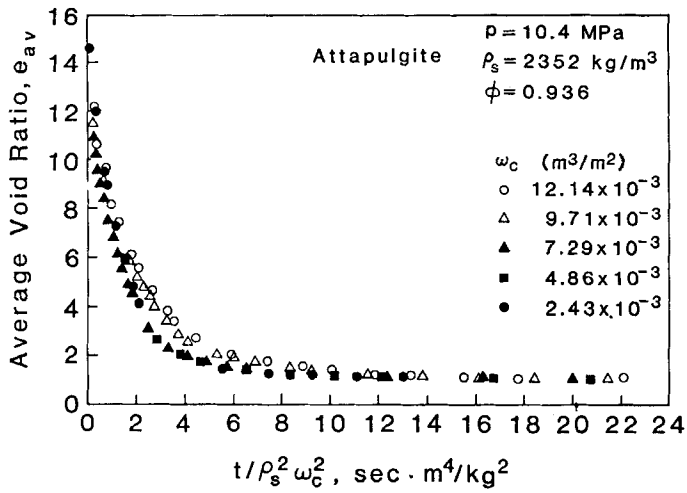

Figure 16. Average void ratio vs. $t/\rho_s^2\omega_c^2$ in expression.

THICKENING AND SEDIMENTATION

Classical design procedures for sizing gravity thickeners have been based on work by Coe and Clevenger (1916), Kynch (1952), and Talmadge and Fitch (1955). All of those methods depend upon flux theory which states that the rate of sedimentation depends uniquely on the concentration of solids. Such an assumption works reasonably well until particulates enter into contact and form a sediment. A number of dissertations have been devoted to flux theory (Javaheri, 1971; Tracy, 1973; Blair, 1976). In these investigations, the theoretical framework suggested by Coe and Clevenger (1916) and Kynch (1952) has veen verified experimentally as long as particles were in a free-fall regime and a structured sediment had not formed. Changes necessary to the original theory have been discussed by Tiller (1981), Fitch (1983), and Chen (1984).

In a commercial operation, sediment of roughly a meter in depth is formed on the bottom of the thickener. At that point, Darcy's law applies and the solids flux is no longer a unique function of the solid concentration. In the compression zone, the solids flux expressed as volume of solid per unit area per unit time is a constant and independent of depth for steady-state flow. Inasmuch as there can be no accumulation of solids or changes in concentration with time, the flux of solids at each height x above the thickener bottom is the same. However, the concentration

changes with depth and is a function of underflow rate and compressibility parameters.

The basic boundary parameters involved in gravity sedimentation are underflow concentration ε_{su}, solids flux in the underflow q_s, and the height L of the compression zone. Other important quanitities are permeability K, local volume fraction of solid ε_s, which is a function of x, viscosity μ, liquid and solid densities, ρ and ρ_s, and gravity, g. Flux theory omits most of these parameters and depends upon the solution of a first-order partial differential equation derived from the law of continuity (conservation of mass). Steady-state thickener theory depends upon the integration of the Darcy equation (Chandler, 1975; Kos, 1977; Dixon, 1980; Knoer, 1983; Chen, 1984). Although flux theory continues to serve a useful purpose, it can never provide all of the desired information for thickeners operating with sediments under compression.

CONTINUOUS THICKENER THEORY

The Darcy equation as normally employed for flow through incompressible beds must be modified for use in thickeners (Shirato et al., 1970). The classical Darcy equation takes the form

$$\frac{dp_L}{dx} = \frac{\mu}{K} q = \frac{\mu}{K} \varepsilon u \tag{8}$$

where q is the superficial velocity and $u = q/\varepsilon$ is the average pore velocity of the liquid. The liquid velocity must be replaced by a velocity of the liquid relative to the moving solids. If the solids are considered to fill the antipores, then the average solid velocity in the antipores is related to the superficial velocity of solids by

$$u_s = q_s/\varepsilon_s \tag{9}$$

Eqn. 8 is then rewritten in Darcy-Shirato form as

$$\frac{dp_L}{dx} = \frac{\mu}{K} \varepsilon (u-u_s) = \frac{\mu\varepsilon}{K} \left(\frac{q}{\varepsilon} - \frac{q_s}{\varepsilon_s}\right) \tag{10}$$

where $(u-u_s)$ represents the relative velocity. Taking x as the distance from the bottom of the thickener upward to an arbitrary point in the sediment, including gravity, and considering the downward velocities of liquid and solid to be positive leads to

$$\frac{dp_L}{dx} + \rho g = -\frac{\mu}{K} \varepsilon \left(\frac{q_s}{\varepsilon_s} - \frac{q}{\varepsilon}\right) \tag{11}$$

The sedimentation velocity of the solids is greater than the downward velocity of the liquid. A force balance similar to the one used in obtaining Eqn. 7 is written over a differential sediment thickness. Inclusion of the weight of the liquid and solid leads to

$$\frac{dp_L}{dx} + \frac{dp_s}{dx} = - g(\rho\varepsilon + \rho_s\varepsilon_s) \tag{12}$$

Combining Eqns. 11 and 12 produces

$$\frac{dp_s}{dx} = - g(\rho_s - \rho)\varepsilon_s + \frac{\mu\varepsilon}{K}\left(\frac{q_s}{\varepsilon_s} - \frac{q}{\varepsilon}\right) \tag{13}$$

As the thickener operates under steady state conditions, the superficial flow rates q_s and q are constant throughout the sediment. We now introduce a number of highly simplified assumptions. The bottom of the thickener is assumed to be flat, i.e., without a slope. The rake is assumed to be infinitely thin and to be revolving at an infinite angular speed. The solid and liquid are removed instantaneously as they reach the bottom, and the underflow concentration of solids is assumed to equal the concentration on the bottom of the thickener (Dixon, 1980, 1981). These assumptions are essentially equivalent to those employed in Coe and Clevenger flux theory. A material balance for the underflow concentration yields

$$\varepsilon_{su} = \frac{q_s}{q_s + q} \tag{14}$$

Solving for q in Eqn. 14 and substituting the result in Eqn. 13 gives

$$\frac{dp_s}{dx} = - g(\rho_s - \rho)\varepsilon_s + \frac{u}{K} q_s \left(\frac{1}{\varepsilon_s} - \frac{1}{\varepsilon_{su}}\right) \tag{15}$$

A simple integration of this equation yields a relationship for a flat-bottomed ideal thickener as follows

$$\int_0^L dx = L = \int_0^{p_{su}} \frac{dp_s}{g(\rho_s - \rho)\varepsilon_s - \frac{u}{K} q_s \left(\frac{1}{\varepsilon_s} - \frac{1}{\varepsilon_{su}}\right)} \tag{16}$$

The actual integration requires definition of conditions at the top and bottom of the sediment. Integration of Eqn. 16 leads to the curves of Fig. 17 where the height of sediment L required to produce a fixed underflow concentration ε_{su} is plotted against underflow rate q_s. If ε_{su} is fixed, then p_{su} as the upper limit of integration in Eqn. 16 is fixed. Numerical integration yields

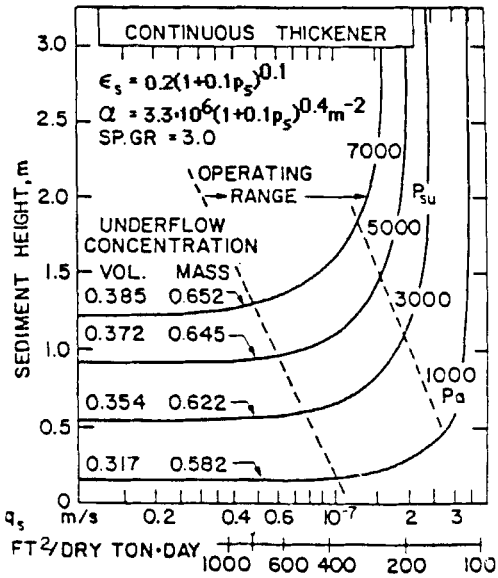

Figure 17. Sediment height vs. p_{su} and q_s in a continuous thickener.

the curves shown in Fig. 17. The solid flow rate is given in basic units of $m^3/m^2.s$ and the practical units of sq.ft./(ton of solids/day).

Each curve is characterized by two asymptotes. The horizontal asymptote corresponds to low production rates and long detention time. The Darcy force is negligible, and the porosity at each level could be calculated by neglecting the drag term in Eqn. 1.

Clearly, the value of the thickened underflow is solely a function of the sediment height. As an approximation for the substance shown in Fig. 17, the underflow concentration is independent of the underflow as long as that flux is about one-third of its maximum value.

The second vertical asymptote occurs at the point of fluidization where an infinite depth of sediment is required to maintain the desired underflow concentration. At this point, the Darcy forces just balance the buoyed weight of the solids which surge into the overflow from the thickener. The rapid raise of the sediment level close to fluidization indicates that the production rate of underflow must be kept at some reasonable value below its maximum for safe operation.

As the underflow concentration is increased, the height of sediment required to maintain a given underflow rate increases, and the sediment fluidization velocity decreases.

Although the calculations have been made for an idealized case with a flat-bottomed thickener and infinitely thin rakes rotating at infinite velocity, the basic trends are similar to those experienced in real units. From an experimental viewpoint, much useful information could be obtained from a knowledge solely of the two asymptotes. In these calculations, it is assumed that the flux demanded by the Talmadge-Fitch (1955) method is sufficient to meet the values used for constructing Fig. 17.

Knoer (1983) developed an experimental technique for determining the two asymptotes of Fig. 17 using an upflow technique through a sedimenting bed. Chen (1984) continued the work of Knoer and is presently making a comprehensive analysis of the thickening equations.

ACKNOWLEDGEMENT

The authors wish to thank the Office of Basic Energy Sciences of the Department of Energy for Grant DE-AS05-81ER-10946 which has enabled them to carry on fundamental research in the theory of solid-liquid separation.

NOMENCLATURE

A	cross-sectional area, m^2
e_{av}	average void ratio (-)
F_s	accumulative drag on particles, N
g	acceleration of gravity, m/s^2
K	Darcy permeability, m^2
K_o	Darcy permeability of unstressed cake, m^2
L	cake thickness, m
n	compressibility coefficient, Eqn. (2), (-)
p	applied pressure, N/m^2
Δp_c	pressure drop across cake, N/m^2
p_a	empirical parameter, N/m^2
p_L	hydraulic pressure, N/m^2
p_s	accumulative drag pressure on solids, $p-p_L$, N/m^2
p_{su}	value of p_s at bottom of thickener, N/m^2
q	superficial liquid flow rate, $m^3/(m^2.s)$
q_s	superficial solid flow rate, $m^3/(m^2.s)$
t	time, s
u	average velocity of liquid in pores, m/s
u_s	average velocity of solids in antipores, m/s
x	distance from medium or bottom of thickener, m

Greek Symbols

α	local specific flow resistance, m^{-2}
α_{av}	average specific flow resistance, m^{-2}
α_o	value of α in unstressed cake, m^{-2}
β	compressibility coefficient, Eqn. (1), (-)
δ	compressibility coefficient, Eqn. (3), (-)
ε	porosity, (-)
ε_{av}	average porosity, (-)
ε_s	volume fraction of solids (solidosity), (-)
ε_{sav}	average volume fraction of solids, (-)
ε_{so}	unstressed value of ε_s, (-)
ε_{su}	volume fraction of solids in the underflow of a continuous thickener, (-)
μ	viscosity, Pa.s
ρ	density of liquid, kg/m^3
ρ_s	true solid density, kg/m^3
ω	volume of dry solids/unit area, m^3/m^2
ω_c	total volume of dry solids/unit area in the cake, m^3/m^2

LITERATURE CITED

1. Blair, D. B., "Dynamics of Continuous Thickening," Ph.D. Disseration, Clemson University, Clemson, SC (1976).

2. Bridger, K., M. Tadros, W. Leu, and F. M. Tiller, "Filtration Behavior of Suspensions of Uniform Polystyrene Particles in Aqueous Media," Sep. Sci. Tech., 18, 1417-1438 (1983).

3. Chandler, J. L., "Design of Deep Thickeners," Preprint, Alcan Jamaica Limited, Mandeville, Jamaica, West Indies (1975).

4. Chen, W., "A Study of the Mechanism of Sedimentation," M.S. Thesis, University of Houston, Houston, TX (1984).

5. Coe, H. S., and C. H. Clevenger, "Methods for Determining the Capacities of Slime-Settling Tanks," Trans. Amer. Inst. Min. Engr., 60, 356-384 (1916).

6. Dixon, D. C., "Effect of Sludge Funneling in Gravity Thickeners," AIChE Journal, 26, 471-477 (1980).

7. Dixon, D. C., "Thickener Dynamic Analysis Accounting for Compression Effects," Chem. Eng. Sci., 36, 499-507 (1981).

8. Fitch, B., "Kynch Theory and Compression Zones," AIChE Journal, 29, 940-947 (1983).

9. Javaheri, A. B., "Continuous Thickening of Aqueous Suspensions," Ph.D. Dissertation, University of Illinois, Urbana, IL (1971).

10. Knoer, P., "Compression Zone Requirement of Gravity Thickeners," M.S. Thesis, University of Houston, Houston, TX (1983).

11. Kos, P., "Fundamentals of Gravity Thickening," Chem. Eng. Progr., 73, 99-105 (Nov., 1977).

12. Kynch, G. J., "A Theory of Sedimentation," Trans. Faraday Soc., 48, 166-176 (1952).

13. Shirato, M., Kato, H. Kobayashi, K., and Sakazaki, H., "Analysis of Settling of Thick Slurries Due to Consolidation," J. Chem. Eng. (Japan), 3, 98-104 (1970).

14. Talmadge, W. P., and E. B. Fitch, "Determining Thickener Unit Areas," Ind. Eng. Chem., 47, 38-41 (1955).

15. Tiller, F. M., "Revision of Kynch Sedimentation Theory," AIChE J., 27, 823-829 (1981).

16. Tiller, F. M. and T. C. Green, "The Role of Porosity in Filtration IX: Skin Effect with Highly Compressible Materials," AIChE J., 19, 1266-1269 (1973).

17. Tiller, F. M., and L. L. Horng, "Hydraulic Deliquoring of Compressible Filter Cakes, Part 1: Reverse Flow in Filter Presses," AIChE J., 29, 297-305 (1983).

18. Tiller, F. M. and W. M. Lu, "The Role of Porosity in Filtration, Part 8, Cake Non-Uniformity in Compression-Permeability Cells," AIChE J., 18, 569-572 (1972).

19. Tiller, F. M. and W. F. Leu, "Basic Data Fitting in Filtration," J. Chinese Inst. Chem. Engr., 11, 64-70 (1980).

20. Tiller, F. M. and C. S. Yeh, "Deposition of Filter Cakes on Radial Surfaces," AIChE J., 31, 1241-1248 (1985).

21. Tracy, K. D., "Mathematical Modeling of Unsteady-State Thickening of Compressible Slurries," Ph.D. Dissertation, Clemson University, Clemson University, Clemson, SC (1973).